

Adaptive Wavelet Transform Based on Artificial Fish Swarm Optimization and Fuzzy C-means Method for Noisy Image Segmentation

Rui Yang^{1,2} and Dahai Li^{1,2}

¹ School of Electronic and Electrical Engineering,
Zhengzhou University of Science and Technology
Zhengzhou, 450015 China
snowycry@qq.com

² Henan Intelligent Information Processing and
Control Engineering Technology Research Center
Zhengzhou, 450015 China
haihaideyou@163.com

Abstract. Aiming at the problem that traditional fuzzy C-means (FCM) clustering algorithm is susceptible to noise in processing noisy images, a noisy image segmentation method based on FCM wavelet domain feature enhancement is proposed. Firstly, the noise image is decomposed by two-dimensional wavelet. Secondly, the edge enhancement of the approximate coefficient is carried out, and the artificial fish swarm (AFS) optimization algorithm is used to process the threshold value of the detail coefficient, and the processed coefficient is reconstructed by wavelet transform. Finally, the reconstructed image is segmented by FCM algorithm. Five typical gray-scale images are selected by adding Gaussian noise and Salt& pepper noise, respectively, and segmented by various methods. The peak signal-to-noise ratio (PSNR) and error rate (MR) of segmented images are used as performance indexes. Experimental results show that compared with traditional FCM clustering algorithm segmentation method, particle swarm optimization (PSO) segmentation method and other methods, the indexes of image segmentation by the proposed method is greatly improved. It can be seen that the proposed segmentation method retains the texture information of image edge well, and its anti-noise performance and segmentation performance are improved.

Keywords: FCM, artificial fish swarm optimization, wavelet transform, noisy image segmentation.

1. Introduction

Image segmentation is a basic pre-processing step to deal with subsequent practical problems, which builds a bridge between initial image processing and later recognition. Image segmentation is to segment an image into object and background. The segmentation process is the grouping process of pixels, which occurs between pixels with similar attributes in the neighborhood, such as intensity, color or texture [1-3].

Noise is an inevitable part of computer vision processing. How to avoid the influence of noise is a significant research direction at present. Fuzzy C-means (FCM) algorithm is a popular image segmentation method at present. A large number of researchers have

carried out researches on noisy image segmentation based on FCM algorithm [4,5]. Compared with the hard segmentation method, FCM algorithm can retain more details of image texture. In view of the weak anti-noise performance of traditional FCM algorithm, relevant scholars propose the methods of combining FCM algorithm with other algorithms to remove noise. Reference [6] proposed a gray image segmentation method based on FCM and artificial bee colony (ABC) optimization. Reference [7-9] proposed an image segmentation method combining particle swarm optimization (PSO) algorithm and FCM. The introduction of PSO algorithm [10], genetic algorithm [11] and gray wolf algorithm [12] improves the robustness of image segmentation to a certain extent. PSO algorithm is easy to fall into local extremum in the search process, and has low convergence accuracy and slow speed in the later stage of evolution. At present, some researchers improve the FCM algorithm to enhance the anti-noise performance of the algorithm. A dynamic parameter FCM image segmentation algorithm based on edge subdivision was proposed in reference [13]. In reference [14], local and non-local information were introduced into the objective function, and the weight between pixel information and non-local spatial information was adjusted by information entropy to enhance the anti-noise performance of the algorithm. The above segmentation methods retain less edge texture information and only improve the anti-noise performance and segmentation performance.

In this paper, based on the traditional FCM image segmentation, a noisy image segmentation method based on wavelet transform is proposed. Firstly, the noisy image is decomposed by two-dimensional wavelet. Secondly, the AFC algorithm is used to process the threshold value of the image detail coefficient, and the edge enhancement of the approximate coefficient is carried out. Then, FCM algorithm is used for image segmentation, so that it can retain more image edge texture information during segmentation.

The rest of the paper is organized as follows. Section 2 and section 3 introduce the related works and preliminaries, including WTF, FCM. Section 4 displays the modified artificial fish swarm algorithm. The proposed noise image segmentation model is proposed in Section 5. The experiments are conducted on section 6, with the conclusion of our manuscript outlined in Section 7.

2. Related Works

Image segmentation is an important process of dividing an image into several regions with similar or identical features (including brightness, color, texture, etc.). In recent years, a variety of image segmentation algorithms have emerged for different application occasions [15]. Clustering method has been widely used in the field of image segmentation [16]. Fuzzy C-Means clustering (FCM) is a soft clustering algorithm based on fuzzy set theory. Different from hard clustering algorithm, each data point has a certain degree of membership for all cluster clusters. Through several iterations, the minimum value of the objective function is found and the cluster cluster with the maximum membership degree of each data point is output. Although FCM clustering algorithm has good segmentation performance for noiseless images, it does not consider information other than pixels, so its segmentation effect for noisy images needs to be improved. Reference [17] proposed a suppression FCM algorithm (S-FCM). Through competitive learning mechanism, the clustering cluster with the largest membership degree was rewarded and other clustering clusters were punished, so as to accelerate the convergence speed of the objective func-

tion and maintain the clustering effect. Reference [18] proposed a Bias Corrected FCM (BCFCM) with the introduction of spatial neighborhood restriction term for the segmentation of medical brain images. With the neighborhood restriction term, it had certain robustness to noise.

Reference [19] proposed a FCM with Generalized Improved Fuzzy Partitions (GIFP-FCM), a membership limit item was added to the objective function of FCM, which improved the classification effect of cluster clusters and the convergence speed. Reference [20] put forward a new Local information restriction term and added it into the FCM objective function, and put forward a Fuzzy Local information C-means (FLICM), which had a good segmentation effect on noise images. Reference [21] proposed a FCM with non-local spatial information by using the image non-local information and the objective function proposed in reference [22] to solve the problem that only considering the local image information was not enough to obtain good segmentation effect, so as to make more effective use of image information. Reference [23] proposed a self-tuning non-local spatial-information FCM algorithm, which could automatically obtain the most appropriate filtering parameters for different pixels and improve the flexibility and robustness of the algorithm. Reference [24] combined the suppressed FCM algorithm with the intuitive fuzzy set for membership degree, removed the suppressed FCM algorithm parameters, and applied non-local spatial information to propose a suppressed non-local spatial intuitive FCM algorithm (SNLS-IFCM). Reference [25] proposed the attribute similarity of 2-element topological subspace, and presented a new FCM based on similarity of attribute space (FCM-SAS). The accuracy of clustering was improved by using membership degree and sample attribute information of clustering center. FCM algorithm based on kernel method is an important method. The kernel method maps the data that is difficult to classify linearly from low dimension to high dimension so as to achieve linear classification of data in high dimension.

Based on the FLICM algorithm, the Kernel method was substituted for Euclidean distance in reference [26], a new fuzzy factor was given, and the Kernel Weighted FLICM (KWFLICM) algorithm was proposed. Based on the constraint factor in the fuzzy factor of KWFLICM algorithm, reference [27] proposed a new weighted image to be used in the constraint term, realized fuzzy clustering by using the Kernel method instead of Euclidean distance, and presented the adaptive constrained Kernel FCM algorithm (Kernel FCM) Fuzzy C-Means. On the basis of KWFLICM, reference [28] extended the clustering object to multidimensional data, sorted and considered the data and neighborhood of each dimension, realized the clustering of multidimensional data by the kernel method, and gave the Generalized KWFLICM algorithm. However, the above methods do not reduce the number of iterations required for convergence of objective function, and the improvement of segmentation efficiency is not obvious.

3. Preliminaries

3.1. Wavelet Transform

Mallat algorithm proposed the concept of multi-resolution analysis. Since digital images are usually represented by two-dimensional array $f(x, y)$, it is assumed that two-dimensional signal is $f(x, y)$, and two-dimensional Mallat algorithm is adopted to carry out wavelet changes [20,30]. The two-dimensional wavelet transform is defined as:

$$WT(a, b_1, b_2) = \frac{1}{a} \int \int f(x, y) \varphi(x, y) dx dy. \quad (1)$$

Where, a is the introduced normalized factor, which ensures the invariable energy before and after wavelet contraction. φ is the Fourier transform. Its inverse transformation is:

$$f(x, y) = \frac{1}{c_\phi} \int_0^{+\infty} \frac{1}{a^3} da \int \int (a, b_1, b_2) \phi(x, y) db_1 db_2. \quad (2)$$

where

$$c_\phi = \frac{1}{4\pi^2} \int \int \frac{|\phi(w_1 + w_2)|^2}{|w_1^2 + w_2^2|} dw_1 dw_2. \quad (3)$$

Digital images are broken down by two-dimensional wave and it gets four components namely, the diagonal coefficient D , horizontal coefficient H , vertical coefficient V and approximate coefficient A respectively. Where D , H , and V are also called detail coefficients.

3.2. Wavelet threshold function

In this paper, soft threshold function [31] is used for value processing of wavelet coefficients, removing or attenuating the coefficients easily damaged by noise and reserving the useful ones so as to suppress noise. The threshold function is as follows:

$$W = \text{sign}(w)(|w| - \lambda), |w| > \lambda. \quad (4)$$

when $W = 0$, $|w| \leq \lambda$. Artificial fish swarm algorithm performs threshold processing on images through Equation (4). Coefficient A does not carry out threshold processing, because coefficient A contains a lot of details useful to the image.

3.3. Adaptive evaluation

The performance of the fish should be evaluated at each generation selection so that the optimal solution can be obtained. The image is reconstructed by inverse wavelet transform with the detail coefficient and approximate coefficient after the threshold processing. Then, the FCM objective function is calculated according to the reconstructed image, as shown in Equation (5), where the data point is the gray value of each pixel point. This fitness evaluation is directly aimed at the segmentation result, and thus indirectly at the image noise.

$$J = \sum_{i=1}^C \sum_{j=1}^L u_{i,j}^m d^2(h, v_i). \quad (5)$$

Although this objective function needs to be calculated in each generation selection of the artificial fish swarm algorithm, the overall calculation cost is within an acceptable range due to the use of histogram based FCM.

3.4. Edge enhancement

Image noise exists in detail coefficient after wavelet decomposition. In order to retain the texture features of image edge, this paper uses Canny edge detection algorithm [32] to detect image edge information by acting on approximate coefficients. Formula (6) is used to realize image enhancement. The two coefficients are reconstructed by wavelet transform to preserve the edge texture features of the image and improve the image segmentation quality effectively.

$$A_f = k \times A + (1 - k) \times A_e. \quad (6)$$

Where, $k \in [0, 1]$ is a constant. A_e is the coefficient processed by Canny edge detection algorithm.

3.5. FCM

FCM algorithm is a fuzzy clustering algorithm based on objective function. In order to make FCM segmentation faster, this paper uses FCM to cluster gray level instead of pixel points. Because the number of gray levels is generally much smaller than the number of pixels. The essence of image segmentation by clustering method is to divide the gray level set into C class. Each class contains unique clustering center, which can be updated in the continuous generation selection, and the clustering result can be optimized by minimizing the objective function. Membership matrix is used to describe the generic properties of each pixel, and the degree of membership of a single pixel in different categories can be judged by its similarity to the cluster center.

The gray level set in the image is $X = x_1, x_2, \dots, x_c$, it divides these data into C categories, then there will be C cluster centers. x_i is a pixel-related feature vector in one-dimensional vector space, and the objective function can be changed to:

$$J = \sum_{i=1}^C \sum_{j=1}^L s_j u_{i,j}^m d^2(j, v_i). \quad (7)$$

Where s_j is the number of pixels with gray level j . L is gray level quantity. m is the membership factor, $m \in (1, +\infty)$. Lagrange multipliers are used to obtain the clustering center renewal equation and the membership equation that minimizes the objective function.

$$u_{i,j}^{k+1} = \frac{1}{\left(\sum_{h=1}^C \left(\frac{d(h, v_i^k)}{d(h, v_m^k)} \right)^{2/(m-1)} \right)}. \quad (8)$$

$$v_i^k = \sum_{l=1}^L (u_{j,i}^k)^m s_j j / \sum_{l=1}^L (u_{j,i}^k)^m s_j. \quad (9)$$

4. Modified artificial fish swarm algorithm

The artificial fish swarm algorithm imitates the characteristics of fish gathering and abstracts the real fish as an artificial fish in the fish swarm algorithm [33,34] to encapsulate

its own state and behavior. By receiving the stimulus information of the external environment, it selects the corresponding activities and affects the external environment through the change of its own state information. The artificial fish interact with each other to find the highest concentrations of food in the environment. During the state change of the artificial fish, the artificial fish may gather in the center of the range with the highest local food concentration. If the state center with the highest food concentration in the environment of all artificial fish is required, other influencing factors are applied to help the artificial fish jump out of the local optimal state center. The local optimal solution of artificial fish swarm algorithm is mainly due to the constant crowding factor which makes the optimal solution deviate from the reality. The moving step size of the artificial fish is fixed, so the artificial fish cannot continue to search for the optimal solution. In this paper, random number is introduced to add random value to step size to help artificial fish jump out of local optimal solution. Constant crowding factor lengthens the optimization time of the algorithm. In this paper, a fitness function is used to reduce the constant crowding factor adaptively so as to shorten the search time of the algorithm and reduce the error between the optimal solution and the actual value.

This paper improves the movement strategy. First, each artificial fish is rear-ended to determine the center with the highest food concentration and update the bulletin board status and the optimal artificial fish status until the artificial fish stops searching forward.

1. AF-follow behavior

If the current moving artificial fish is X_i , it searches f_i with the highest concentration of food near the artificial fish corresponding to another artificial fish X_j with the largest concentration. If $f_i/n_f = \sigma f_i$, it indicates that there is a high food concentration in the position of X and the surrounding environment of the artificial fish is not crowded, then the artificial fish moves forward in the direction of X_j , otherwise the foraging behavior is performed. This behavior is used to speed up the movement of the artificial fish to a better state.

Let $f_{max} = f_i$, $X_{max} = X_j$, it can obtain the artificial fish X_i forward position.

$$X_{next} = \frac{X_i + (X_{max} - X_i)}{\|X_i + (X_{max} - X_i)\|} \cdot step \cdot Rand(). \quad (10)$$

If the artificial fish stops searching, the foraging behavior of the artificial fish is performed, and the bulletin board and the best artificial fish are selected and updated.

2. AF-prey behaviour

Setting the current artificial fish state as X_i , selecting a state X_j in its visual range,

$$X_j = X_i + visual \cdot Rand(). \quad (11)$$

Judging whether the conditions of artificial fish moving forward are satisfied. Until the artificial fish meets the search times. If the forward condition is still not met, moving one step randomly according to equation (12).

$$X_i^{t+1} = X_i^t + step \cdot Rand(). \quad (12)$$

If the artificial fish stops searching in the above two steps, the clustering behavior will be performed until the iteration termination condition is satisfied.

3. AF-swarm behaviour.

If the current artificial fish status is X_i , it searches for the number of fish n_f near artificial fish X_i and the central location X_c with the highest food concentration. If there is $f_c/n_f = \sigma f_i$, it indicates that the food concentration in the center of the shoal is high and not crowded, and the artificial fish X_i moves forward to the center of the shoal. This behavior is used to make a few artificial fish trapped in the local optimal solution tend to the direction of the global optimal solution.

$$X_{next} = X_i + \frac{X_c - X_i}{\|X_c - X_i\|} \cdot step \cdot Rand(). \tag{13}$$

Otherwise, it performs foraging behavior.

The process of improving artificial fish swarm algorithm is shown in figure 1. Firstly, the total number of fish N and the number of generations selected by the artificial fish swarm algorithm are set to calculate the food concentration of each artificial fish in the current fish swarm. The artificial fish with the highest food concentration is selected as the optimal artificial fish in the current fish swarm. It initializes the state of the best artificial fish as the value of the bulletin board. Combined with the selection times of fish swarm optimization, the moving step size of artificial fish is improved, and the weight is introduced to the step size of artificial fish to solve the problem of convergence speed of the algorithm. According to the characteristics of fish movement, the algorithm chooses to carry out tail-chasing and foraging behaviors first, aiming to enable fish to quickly determine the center position with high food concentration, and then carries out the movement strategy of fish clustering behavior, aiming to avoid overcrowding between fish and adjacent artificial fish and improve the ability of artificial fish to get rid of local optimal solution. According to the above moving strategy, each artificial fish should perform the following operations, such as chasing behavior, clustering behavior and foraging behavior, and update the content of the optimal artificial fish and bulletin board iteratively until the average value obtained for several consecutive times does not exceed the sought extreme value or reaches the maximum number of generations. According to the optimal value saved on the bulletin board, the optimal weight matrix is calculated as the basis for setting the initial parameters of the wavelet function.

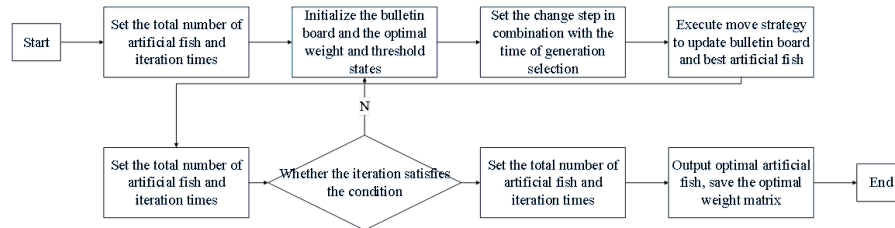


Fig. 1. Optimization process of AF

5. Proposed noise image segmentation

If FCM algorithm segments noise image directly, the segmentation effect is seriously affected by the image noise. Therefore, this paper first uses wavelet transform and AF algorithm fusion to reduce image noise and enhance image edge texture information. Then the reconstructed image is segmented by FCM to make the segmented image more robust. The flow of the proposed method is shown in figure 2.

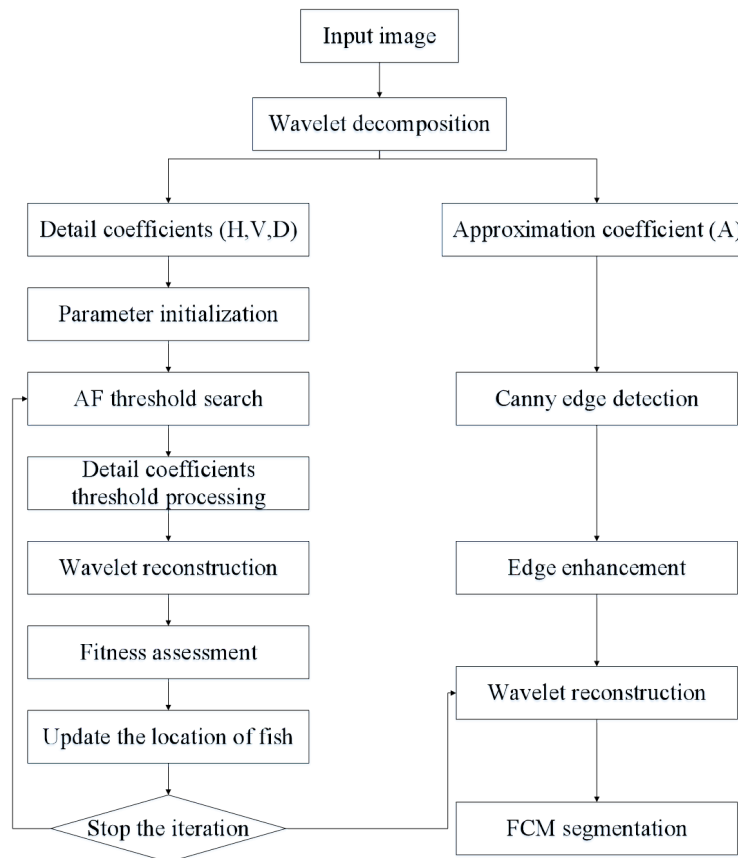


Fig. 2. Flow chart of proposed method

The method in this paper can be divided into four steps as follows.

Step 1. Input the image, perform wavelet decomposition for the image and obtain 4 coefficients:

$$W(X) \rightarrow (A, H, V, D). \quad (14)$$

Where W denotes the wavelet decomposition.

Step 2. AF algorithm is used to search the threshold values of detail coefficients D , H and V respectively. When the fitness value does not exceed the given wide value, the generation selection is stopped after 20 times. After each generation selection, the fuzzy coefficient is processed according to the current threshold, and then the fuzzy coefficient and the unprocessed detail coefficient are reconstructed by wavelet. The reconstructed image is evaluated according to equation (5), which ensures the optimal threshold.

Step 3. Edge enhancement is performed on the fuzzy coefficient A , and the specific expression is shown in Equation (6).

Step 4. The coefficients are reconstructed by wavelet transform, and the reconstructed image is segmented by FCM.

$$W^{-1}(H', V', D', A_f) \rightarrow \hat{X}. \quad (15)$$

$$FCM(X) \rightarrow X_n. \quad (16)$$

Where W^{-1} is the inverse wavelet transform, used to reconstruct the image.

6. Experiments and analysis

In order to verify the segmentation performance and noise suppression ability of the proposed method, five typical grayscale images are selected and named img1, img2, img3, img4, img5 respectively, as shown in figure 3. Gaussian noise and salt and pepper noise are added to the five images respectively. Firstly, the coefficient k in image edge enhancement are set to 0.5, 0.7 and 0.9, respectively. Then, img1 is reconstructed and segmented. The appropriate k value is selected by directly observing the reconstructed and segmented images. The clustering number C is set to 3, 5 and 6 for img4 segmentation experiment. The classification effect and convergence rate of objective function are analyzed, and the appropriate C value is selected. Finally, the proposed method, traditional FCM method and particle swarm optimization algorithm are used for segmentation, and three different results are obtained. The peak signal-to-noise ratio (PSNR) and misclassification rate are used to quantitatively evaluate the anti-noise performance and segmentation performance of the proposed algorithm, and the running time is used to evaluate the time complexity of the algorithm.

The experiment is carried out under Windows10 system, with AMD Ryzen5 2600 CPU, main frequency 3.40 GHz, and 16 GB operating memory. The experimental environment is Matlab a2017 version.

Table 1 shows the image reconstruction and segmentation effects under different k values. It shows that when $k = 0.9$, the reconstructed image texture is the clearest and the segmentation effect is the best.

Figure 4 and figure 5 are the segmentation results of the five images with different noises by using the method in this paper, FCM algorithm and artificial fish swarm algorithm. By directly observing the segmentation results, it can be seen that the image segmented by the proposed algorithm is less affected by noise, especially the segmentation effect of the image containing salt and pepper noise is significantly improved compared with the other two methods, and the proposed algorithm maintains a certain stability under these two kinds of noise.

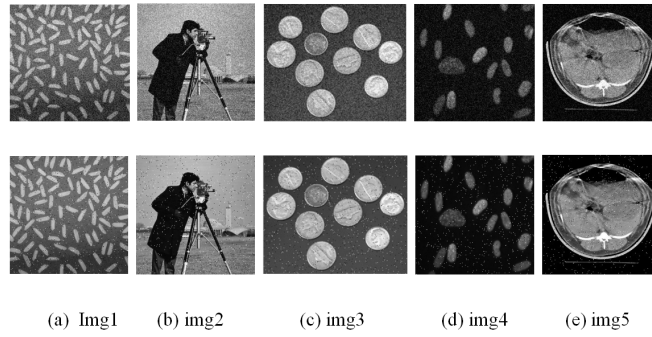


Fig. 3. Original and noise added images. The first row is added Gaussian noise and the second row is added salt & pepper noise.

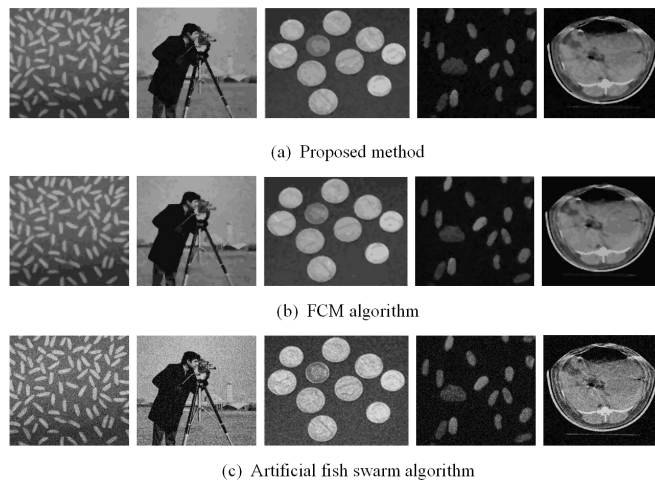
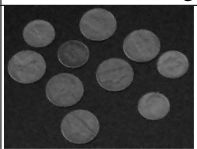
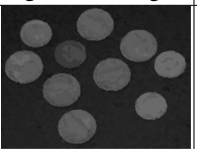
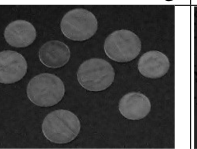
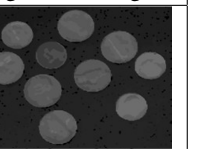
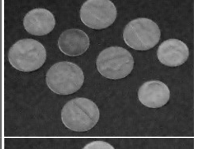
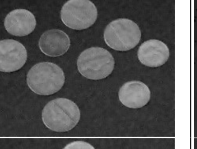
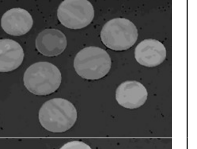
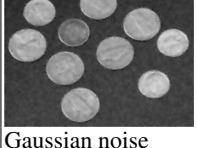
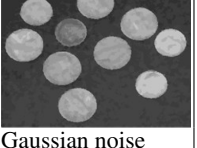
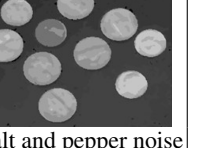


Fig. 4. segmentation results with Gaussian noise

Table 1. Comparison of image reconstruction effect and segmentation effect with different k values

k value	Reconstructed image	Segmented image	Reconstructed image	Segmented image
k=0.5				
k=0.7				
k=0.9				
k value	Gaussian noise	Gaussian noise	salt and pepper noise	salt and pepper noise

In order to further verify the anti-noise performance of the proposed method, the paper adopts the Peak signal-to-noise Ratio (PSNR) for quantitative evaluation [35]. The larger PSNR denotes the better the anti-noise performance of the proposed method, which is defined as:

$$PSNR = 10lg(MAX^2/MSE). \tag{17}$$

Where MAX is the maximum value of image pixels. MSE is the mean square error of image pixels and is defined as:

$$MSE = \frac{1}{mn} \sum_{i=1}^n \sum_{j=1}^m ||K(i, j) - I(i, j)||^2. \tag{18}$$

Where mn is the size of the image. K and I are the original noisy image and the segmented image respectively.

In order to further verify the segmentation performance of the proposed method, Misclassification Error (ME) is used as an indicator to evaluate the segmentation performance of the proposed method. The smaller ME value denotes the better segmentation performance of the proposed method, which is defined as:

$$ME = (1 - \sum_{i=1}^C A_i \cap B_j (\sum_{j=1}^C B_j)^{-1}) \times 100\%. \tag{19}$$

Where A_i represents the pixel points divided into class i in the segmentation algorithm. B_j represents the pixels divided into class j in an ideal image without noise. C is the number of categories.

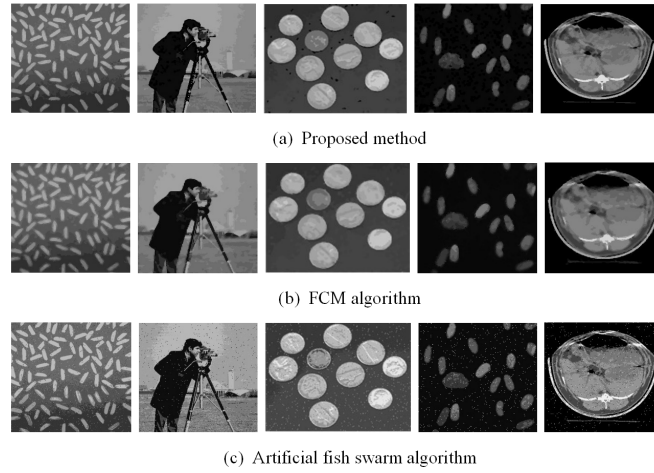


Fig. 5. Segmentation results with salt and pepper noise

In order to objectively evaluate the anti-noise performance and segmentation performance of the segmentation method in this paper, The PSNR value and ME value of segmented images by three methods are given in Table 2. The PSNR value and ME value of segmented images by these three methods are compared and analyzed. The PSNR value of the segmented images by this method is 16% and 20% higher than that of traditional FCM segmentation method and AF algorithm segmentation method on average. ME values decrease by 28% and 13% on average, respectively. The proposed method has better segmentation performance for noisy images and better anti-noise performance. However, compared with the traditional FCM method, the running time of the proposed algorithm is longer than that of the traditional FCM method, which has a slight advantage over the AF algorithm segmentation method.

The following contents are the comparison results with state-of-the-arts image segmentation methods including ACMAWF [36], ACMFR [37], RFRBSFCM [38], PDB-SCAN [39]. Here, mean Intersection over Union (mIoU) and Normalized Mutual Information (NMI) are used to evaluate the effectiveness of the proposed method.

$$mIoU = \frac{1}{K} \sum_{i=1}^K (A_i \cap C_i) / (A_i \cup C_i). \quad (20)$$

Where A_i is the pixel set of the i -th cluster in the segmentation result. C_i is the pixel set of the i -th cluster in the reference image. Larger mIoU indicates better segmentation effect. For gray image I_1 and gray image I_2 ,

$$NMI = 2MI(I_1, I_2) / [H(I_1) + H(I_2)]. \quad (21)$$

Where, I_1 and I_2 have the same size, $MI(I_1, I_2)$ represents the mutual information of I_1 and I_2 . $H(I_1)$ and $H(I_2)$ represent the entropy of I_1 and I_2 respectively. The larger NMI denotes the better segmentation result.

Table 2. PSNR, ME and time consumption of noisy image segmentation by three methods

Method	Images	Noisy image	PSNR/dB	ME	Time/s
FCM	Img1	Gaussian noise	4.2751	0.4744	1.102
FCM	Img1	salt and pepper noise	6.6731	0.4032	1.068
FCM	Img2	Gaussian noise	3.3621	0.4891	1.081
FCM	Img2	salt and pepper noise	7.8971	0.4161	1.094
FCM	Img3	Gaussian noise	5.3441	0.3871	1.242
FCM	Img3	salt and pepper noise	7.6271	0.4251	1.227
FCM	Img4	Gaussian noise	6.3481	0.3541	0.091
FCM	Img4	salt and pepper noise	7.2451	0.3961	1.103
FCM	Img5	Gaussian noise	4.4531	0.3922	1.104
FCM	Img5	salt and pepper noise	5.9599	0.3631	1.730
Proposed method	Img1	Gaussian noise	13.7831	0.2161	1.752
Proposed method	Img1	salt and pepper noise	14.8771	0.2241	1.711
Proposed method	Img2	Gaussian noise	12.4991	0.3341	1.793
Proposed method	Img2	salt and pepper noise	16.2786	0.2998	1.724
Proposed method	Img3	Gaussian noise	15.7391	0.3151	1.778
Proposed method	Img3	salt and pepper noise	16.5051	0.2847	1.786
Proposed method	Img4	Gaussian noise	16.5051	0.2847	1.786
Proposed method	Img4	salt and pepper noise	14.1941	0.3271	1.862
Proposed method	Img5	Gaussian noise	13.5921	0.3281	1.925
Proposed method	Img5	salt and pepper noise	15.9681	0.2971	1.833
AF	Img1	Gaussian noise	10.6561	0.3251	1.756
AF	Img1	salt and pepper noise	9.6499	0.3781	1.732
AF	Img2	Gaussian noise	9.9531	0.3531	1.735
AF	Img2	salt and pepper noise	13.7861	0.3261	1.717
AF	Img3	Gaussian noise	12.4921	0.3471	1.748
AF	Img3	salt and pepper noise	14.7591	0.3541	2.107
AF	Img4	Gaussian noise	14.4941	0.2971	1.686
AF	Img4	salt and pepper noise	14.1981	0.4291	1.982
AF	Img5	Gaussian noise	12.9951	0.3351	1.916
AF	Img5	salt and pepper noise	12.6971	0.3261	1.891

First, we segment the artificial grayscale image, as shown in Figure 6(a). The image size is 256×256 pixels with 5%, 10%, 15% and 20% noise. Figure 6 shows the segmentation results of artificial images containing 5% mixed noise by five algorithms. The quantitative index results of artificial images are shown in Table 3.

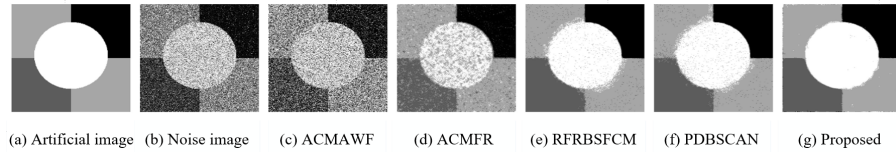


Fig. 6. Segmentation results of artificial images containing 5% mixed noise by five algorithms

Table 3. Segmentation results of artificial images with different mixed noises by five algorithms%

Index	mIoU	mIoU	mIoU	mIoU	NMI	NMI	NMI	NMI
Noise	5	10	15	20	5	10	15	20
ACMAWF	53.76	49.59	36.52	31.52	26.45	15.53	9.20	7.24
ACMFR	86.06	65.36	56.27	50.62	74.43	51.21	39.82	32.01
RFRBSFCM	97.46	88.51	69.57	49.91	87.04	78.08	54.74	39.21
PDBSCAN	97.78	89.86	71.23	55.70	87.11	80.29	58.94	41.24
Proposed	97.81	96.65	93.51	87.82	93.34	90.99	85.46	75.95

The experimental results show that the ACMAWF algorithm has the fastest segmentation speed and poor segmentation effect, and the ACMFR algorithm has improved the segmentation result compared with ACMAWF due to the consideration of local spatial information, but it is not easy to converge. RFRBSFCM and PDBSCAN algorithms use original non-local spatial information, and the latter is superior to the former due to the consideration of intuitive fuzzy sets and membership competitive punishment. In the case of 5% mixed noise, the number of generation selection of PDBSCAN algorithm is less than that of RFRBSFCM algorithm, but when the mixed noise increases to more than 10%, the convergence speed of PDBSCAN algorithm is slower than that of RFRBSFCM algorithm. The segmentation results of the proposed algorithm are better than those of other comparison algorithms, which shows that the proposed algorithm has good segmentation ability and detail retention ability.

The gray scale natural images are segmented with noise. The original images are gear images (263×264 pixels), 42049, 86016 and 118035, respectively. The last three images come from Berkeley image segmentation data set with the size of 481×321 pixels. We add 5%, 10%, 15% and 20% mixed noise to four images respectively. Figures 7 9 and Table 4 compare the segmentation effects and quantitative indexes by five algorithms for four natural images. In Table 4, for each segmentation algorithm, from top to bottom are the

segmentation quantitative index results of gear image, 42049, 86016 and 118035 under different mixed noises.

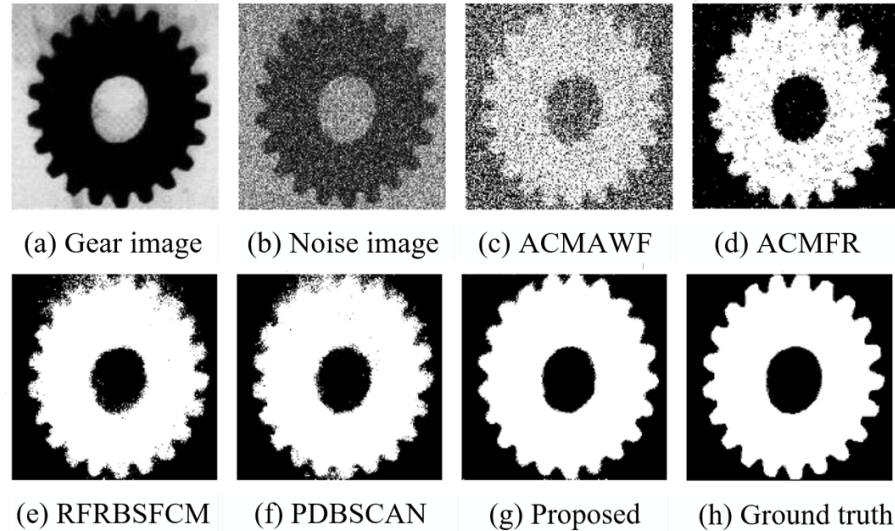


Fig. 7. Segmentation results with five algorithms containing 10% mixed noise for gear image

Experimental results show that because ACMAWF does not consider any image spatial information, the computational complexity is low, the segmentation effect is poor, and the segmentation speed is fastest. In the case of 5% mixed noise and excluding ACMAWF, the segmentation results of binary image by each algorithm are similar. When the intensity of mixed noise increases, ACMFR algorithm degrades the segmentation result of three classification images more than the other four algorithms. The segmentation result of RFRBSFCM is similar to that of PDBSCAN. Due to the original non-local spatial information calculation method, the segmentation time of both is longer. The segmentation result of the proposed algorithm has a small advantage over other algorithms under 5% mixed noise. With the addition of large mixed noise, the segmentation results of the proposed algorithm are better than those of other algorithms.

We also analyze the time complexity of these algorithms. Firstly, the calculation step expression E of the algorithm objective function is calculated. Secondly, all variables in E are unified as variable n , and the calculation step function $E(n)$ is obtained. Finally, let n approaches infinity, find an auxiliary function $f(n)$, so that $f(n)/E(n) = a$, then $E(n)$ and $f(n)$ are the same order of magnitude. $O[f(n)]$ is the time complexity of the algorithm, where a is a constant greater than 0.

In Table 4, H and W are the height and width of the image respectively. K is the number of clusters, $iter$ is the number of generation selection. k is the neighborhood side length of ACMAWF algorithm. S and s are the side length of the search area and the neighborhood side length of the non-local mean filter respectively. ACMFR needs to con-

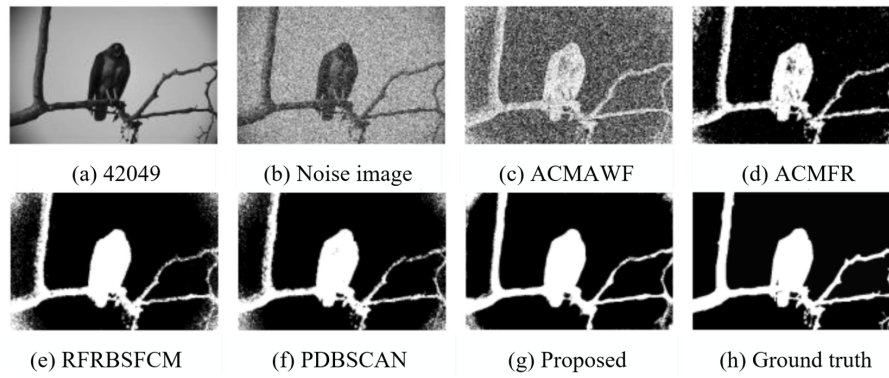


Fig. 8. Segmentation results with five algorithms containing 10% mixed noise for 42049

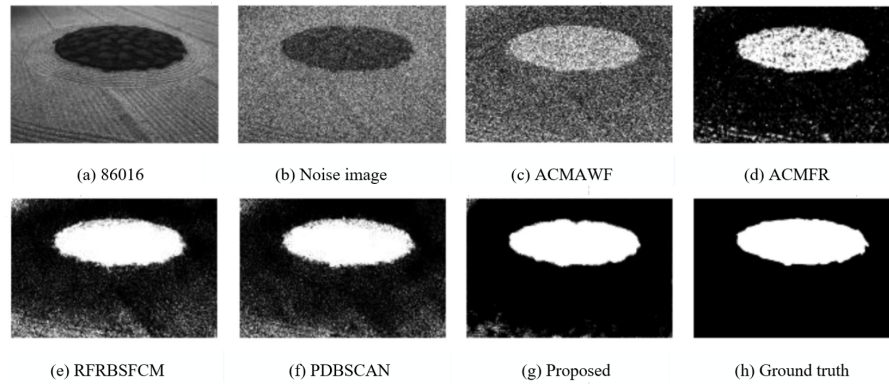


Fig. 9. Segmentation results with five algorithms containing 10% mixed noise for 86016

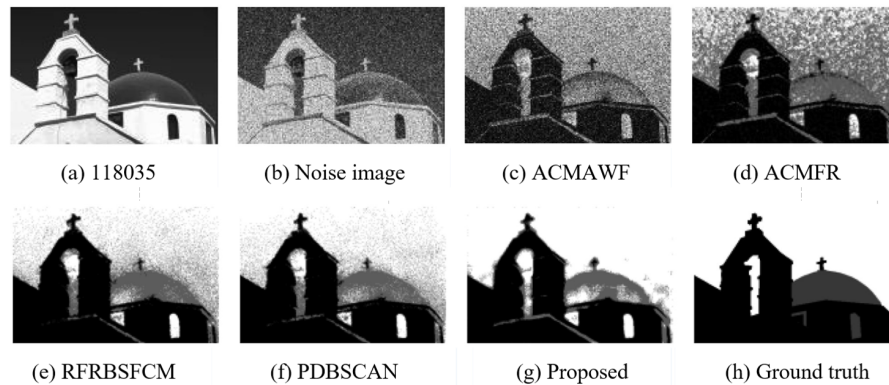


Fig. 10. Segmentation results with five algorithms containing 10% mixed noise for 118035

Table 4. Segmentation results of images with different mixed noises by five algorithms (%)

Index	mIoU	mIoU	mIoU	mIoU	NMI	NMI	NMI	NMI
Noise	5	10	15	20	5	10	15	20
ACMAWF (gear)	83.71	69.99	59.93	55.52	56.10	32.53	18.91	13.43
ACMAWF (42049)	52.27	43.85	39.85	37.37	16.85	8.67	5.61	4.13
ACMAWF (86016)	42.07	37.63	35.14	33.15	9.30	4.38	3.33	2.44
ACMAWF (118035)	37.61	31.84	29.33	13.46	20.56	11.07	7.22	5.23
ACMFR (gear)	98.79	97.38	94.63	90.47	91.91	87.55	80.01	70.14
ACMFR (42049)	87.42	82.03	76.50	72.01	64.92	53.97	43.57	35.74
ACMFR (86016)	79.70	79.21	66.56	62.19	54.02	47.12	29.13	21.09
ACMFR (118035)	47.46	40.31	31.96	26.10	50.12	38.92	28.32	21.58
RFRBSFCM (gear)	98.79	97.46	95.95	93.09	92.08	88.05	84.01	77.73
RFRBSFCM (42049)	87.37	83.50	66.48	52.60	64.80	56.53	32.28	18.38
RFRBSFCM (86016)	89.11	66.23	51.99	43.84	71.96	38.45	22.26	22.88
RFRBSFCM (118035)	68.59	61.19	53.42	42.95	63.93	56.47	45.74	37.54
PDBSCAN (gear)	98.94	97.25	95.81	92.40	92.54	87.51	83.61	76.62
PDBSCAN (42049)	90.75	83.97	68.12	53.67	74.68	57.78	34.14	19.59
PDBSCAN (86016)	90.87	66.62	52.32	43.60	80.92	42.66	23.10	13.34
PDBSCAN (118035)	71.91	60.98	52.83	44.97	66.89	55.26	45.83	36.27
Proposed (gear)	98.00	99.23	97.66	96.30	95.01	93.18	88.81	84.65
Proposed (42049)	97.15	85.66	84.56	83.26	88.12	62.17	59.38	56.99
Proposed (86016)	97.42	93.45	92.49	79.21	88.90	79.43	76.55	54.26
Proposed (118035)	73.86	67.38	68.96	61.14	70.95	66.69	64.24	55.57

sider the $k \times k$ neighborhood of each pixel and membership degree in each generation selection, so the time complexity is $O(n^6)$. Both RFRBSFCM and PDBSCAN algorithms use the original NLM filter, so the time complexity is mainly affected by the time complexity of NLM filter, which is $O(n^6)$. Table 4 shows that the time complexity of the algorithm in this paper is lower, which is $O(n^4)$.

7. Conclusion

The noise image is decomposed by two-dimensional wavelet, then the AF algorithm is used to process the threshold value of the detail coefficient. The approximate coefficients are enhanced by edge enhancement. Finally, the FCM algorithm is used to segment the image. In this paper, Gaussian noise and salt-and-pepper noise are added to five different images, and these images with noise are segmented by the proposed method, traditional FCM method and AF algorithm, respectively. The peak signal-to-noise ratio and misclassification rate of the segmented images are taken as performance indicators. Experimental results show that the proposed method can effectively preserve the edge features of images, and has good anti-noise performance and segmentation performance.

Table 5. Time complexity analysis

Method	E	$E(n)$	Time complexity
ACMAWF	$H \times W \times K \times iter$	n^4	$O(n^4)$
ACMFR	$H \times W \times K \times k^2 \times iter$	n^6	$O(n^6)$
RFRBSFCM	$H \times W \times (2S + 1)^2 \times (2s + 1)^2$ $+ H \times W \times K \times iter$	$n^2(n + 1)^4 + n^4$	$O(n^6)$
PDBSCAN	$H \times W \times (2S + 1)^2 \times (2s + 1)^2$ $+ H \times W \times (K - 1) \times iter$	$n^2(n + 1)^4 + n^4(n - 1)$	$O(n^6)$
Proposed	$H \times W \times [(2S + 1)^2 - 1]$ $+ (2HW) \times K \times iter$	$n^2[(n + 1)^2 - 1] + 2n^4$	$O(n^4)$

References

1. D. Fung, Q. Liu, J. Zammit, K. S. Leung and P. Hu. "Self-supervised deep learning model for COVID-19 lung CT image segmentation highlighting putative causal relationship among age, underlying disease and COVID-19," *Journal of Translational Medicine*, vol. 19, no. 1. (2021)
2. Q. W. Shi, S. L. Yin, K. Wang, L. Teng and H. Li. "Multichannel convolutional neural network-based fuzzy active contour model for medical image segmentation," *Evolving Systems*, (2021) <https://doi.org/10.1007/s12530-021-09392-3>
3. L. Duan, S. Yang, D. Zhang. "Multilevel thresholding using an improved cuckoo search algorithm for image segmentation," *The Journal of Supercomputing*, vol. 77, no. 7, pp. 6734-6753. (2021)
4. X. Xie , Q. Zhang. "An edge-cloud-aided incremental tensor-based fuzzy c-means approach with big data fusion for exploring smart data," *Information Fusion*, vol. 76, no. 5. (2021)
5. S. L. Yin, Y. Zhang, S. Karim. Large Scale Remote Sensing Image Segmentation Based on Fuzzy Region Competition and Gaussian Mixture Model," *IEEE Access*, vol. 6, pp. 26069-26080. (2018)
6. X. Lei and H. Ouyang. "Kernel-Based Intuitionistic Fuzzy Clustering Image Segmentation Based on Grey Wolf Optimizer With Differential Mutation," *IEEE Access*, vol. 9, pp. 85455-85463. (2021)
7. L. Frigau, C. Conversano, F. Mola. "Consistent validation of gray-level thresholding image segmentation algorithms based on machine learning classifiers," *Statistical Papers*, vol. 62. (2021)
8. Z. Zhao, Z. Zeng, K. Xu, C. Chen and C. Guan. "DSAL: Deeply Supervised Active Learning From Strong and Weak Labelers for Biomedical Image Segmentation," *IEEE Journal of Biomedical and Health Informatics*, vol. 25, no. 10, pp. 3744-3751. (2021)
9. X. Zheng, T. Chen. "High spatial resolution remote sensing image segmentation based on the multiclassification model and the binary classification model," *Neural Computing and Applications*, (2021).
10. G. An et al. "Short-Term Wind Power Prediction Based On Particle Swarm Optimization-Extreme Learning Machine Model Combined With Adaboost Algorithm," *IEEE Access*, vol. 9, pp. 94040-94052. (2021)
11. B. Chen, Y. Niu and H. Liu. "Input-to-State Stabilization of Stochastic Markovian Jump Systems Under Communication Constraints: Genetic Algorithm-Based Performance Optimization," *IEEE Transactions on Cybernetics*, (2021) doi: 10.1109/TCYB.2021.3066509.
12. A. Nd, B. Mk, C. Xi, et al. "Towards robust partially supervised multi-structure medical image segmentation on small-scale data," *Applied Soft Computing*, vol. 114. (2021)

13. H. Abdellahoum, N. Mokhtari, A. Br Ahimi, et al. "CSFCM: An improved fuzzy C-Means image segmentation algorithm using a cooperative approach," *Expert Systems with Applications*, 166:114063. (2021)
14. D. Chen, S. Yongchareon, E. Lai, J. Yu and Q. Z. Sheng. "Hybrid Fuzzy C-Means CPD-Based Segmentation for Improving Sensor-Based Multiresident Activity Recognition," *IEEE Internet of Things Journal*, vol. 8, no. 14, pp. 11193-11207. (2021)
15. J. Fan and B. Lei. "Image thresholding segmentation method based on reciprocal rough entropy," *Journal of Electronics & Information Technology*, vol. 42, no. 1, pp. 214-221. (2020)
16. W. Seema, B. Keshavamurthy. "A survey on image data analysis through clustering techniques for real world applications," *Journal of Visual Communication and Image Representation*, vol. 55, pp. 596-626. (2018)
17. Z. Zhu, Y. Liu, Z. Zhao, et al. "Improved suppressed fuzzy c-means clustering algorithm for segmenting the non-destructive testing image," *Chinese Journal of Scientific Instrument*, vol. 40, no. 8, pp. 110-118. (2019)
18. D. Wei, Z. Wang, L. Si, et al. "An image segmentation method based on a modified local-information weighted intuitionistic Fuzzy C-means clustering and Gold-panning Algorithm," *Engineering Applications of Artificial Intelligence*, vol. 101, no. 3, pp. 104209. (2021)
19. M. Kaushal, QMD Lohani. "Generalized intuitionistic fuzzy c-means clustering algorithm using an adaptive intuitionistic fuzzification technique," *Granular Computing*, vol. 1, pp. 183-195. (2021)
20. Z. Yang, P. Xu, Y. Yang, et al. "Noise robust intuitionistic fuzzy c-means clustering algorithm incorporating local information," *IET Image Processing*, vol. 15, no. 3, pp. 805-813. (2021)
21. H. Liu, F. Zhao. "Multiobjective fuzzy clustering with multiple spatial information for Noisy color image segmentation," *Applied Intelligence*, vol. 5, pp. 5280-5298. (2021)
22. Y. Li and Y. Shen. "Robust Image Segmentation Algorithm Using Fuzzy Clustering Based on Kernel-Induced Distance Measure," *2008 International Conference on Computer Science and Software Engineering*, 2008, pp. 1065-1068, doi: 10.1109/CSSE.2008.694.
23. H. Zhang, J. Liu. "Fuzzy c-means clustering algorithm with deformable spatial information for image segmentation," *Multimedia Tools and Applications*, vol. 81, no. 8, pp. 11239-11258. (2022)
24. X. Jia, T. Lei, X. Du, S. Liu, H. Meng and A. K. Nandi. "Robust Self-Sparse Fuzzy Clustering for Image Segmentation," *IEEE Access*, vol. 8, pp. 146182-146195, (2020).
25. W. Shi, J. Zhuo, Y. Lan, et al. "A Novel Fuzzy Clustering Algorithm Based on Similarity of Attribute Space," *Journal of Electronics & Information Technology*, vol. 41, no. 11, pp. 2722-2728. (2019)
26. M. Gong, Y. Liang, J. Shi, et al. "Fuzzy C-Means Clustering With Local Information and Kernel Metric for Image Segmentation," *IEEE Transactions on Image Processing*, vol. 22, no. 2, pp. 573-584. (2013)
27. I. Cherfa, A. Mokraoui, A. Mekhmoukh and K. Mokrani. "Adaptively Regularized Kernel-Based Fuzzy C-Means Clustering Algorithm Using Particle Swarm Optimization for Medical Image Segmentation," *2020 Signal Processing: Algorithms, Architectures, Arrangements, and Applications (SPA)*, 2020, pp. 24-29, doi: 10.23919/SPA50552.2020.9241242.
28. Memon, Kashif, Hussain, et al. "Generalised kernel weighted fuzzy C-means clustering algorithm with local information," *Fuzzy Sets And Systems*, vol. 340, no. 1, pp. 91-108. (2018)
29. H. B. Seidel, M. M. A. da Rosa, G. Paim, E. A. C. da Costa, S. J. M. Almeida and S. Bampi. "Approximate Pruned and Truncated Haar Discrete Wavelet Transform VLSI Hardware for Energy-Efficient ECG Signal Processing," *IEEE Transactions on Circuits and Systems I: Regular Papers*, vol. 68, no. 5, pp. 1814-1826. (2021)
30. A. Hy, B. Yang, C. Rw, et al. "Associations between trees and grass presence with childhood asthma prevalence using deep learning image segmentation and a novel green view index," *Environmental Pollution*, (2021)

31. A. Dz, A. Bh, G. Xun, et al. "ASS-GAN:Asymmetric Semi-supervised GAN for Breast Ultrasound Image Segmentation," *Neurocomputing*, (2022).
32. A. R. Beeravolu, S. Azam, M. Jonkman, B. Shanmugam, K. Kannoopatti and A. Anwar. "Pre-processing of Breast Cancer Images to Create Datasets for Deep-CNN," *IEEE Access*, vol. 9, pp. 33438-33463. (2021)
33. Gao H, Jun-Wei Z. "Estimation of pile settlement applying hybrid radial basis function network with BBO, ALO, and GWO optimization algorithms," *Journal of Applied Science and Engineering*, vol. 25, no. 6, pp. 1031-1044, 2022.
34. Ibrahim, J., Gajin, S. "Entropy-based Network Traffic Anomaly Classification Method Resilient to Deception," *Computer Science and Information Systems*, Vol. 19, No. 1, pp. 87-116. (2022).
35. A. Skd, B. Kd et al. "Opposition-based Laplacian Equilibrium Optimizer with Application in Image Segmentation using Multilevel Thresholding," *Expert Systems with Applications*, vol. 174, (2021)
36. A. Joshi, M.S. Khan, A. Niaz, et al. "Active Contour Model with Adaptive weighted function for Robust Image Segmentation under Biased Conditions," *Expert Systems with Applications*, vol. 175, (2021).
37. J. Fang, H. Liu, J. Liu, et al. "Fuzzy region-based active contour driven by global and local fitting energy for image segmentation," *Applied Soft Computing*, vol. 100, (2021).
38. A. Srinivasan, S. Sadagopan. "Rough fuzzy region based bounded support fuzzy C-means clustering for brain MR image segmentation," *Journal of Ambient Intelligence and Humanized Computing*, vol. 12, pp. 3775-3788, (2021).
39. C. L. Seng, B.A. Macdonald, M. Parsons, et al. "Accelerated superpixel image segmentation with a parallelized DBSCAN algorithm," *Journal of Real-Time Image Processing*, vol. 11, pp. 1-16 (2021).

Rui Yang is with the School of Electronic and Electrical Engineering, Zhengzhou University of Science and Technology, Zhengzhou, 450015 China. Research direction: image processing and cloud computing.

Dahai Li is with the School of Electronic and Electrical Engineering, Zhengzhou University of Science and Technology, Zhengzhou, 450015 China. Research direction: image processing.

Received: March 21, 2022; Accepted: September 15, 2022.